

# Simulation of thin film gas sensors kinetics

V. Brynzari, G. Korotchenkov<sup>\*</sup>, S. Dmitriev

*Department of Microelectronics, Technical University of Moldova, Bld. Stefan cel Mare, 168, Chisinau, 2004, Moldova*

Received 15 September 1998; received in revised form 11 August 1999; accepted 16 August 1999

## Abstract

The consistent approach to simulation of oxygen sensitivity of undoped tin dioxide thin films in transient case was developed. The fundamentals of the model are the physical ideas, which take into consideration the presence of chemisorbed particles in neutral and charged forms on the semiconductor surface. From the analysis of rate equations for dissociative adsorption, the general expression for surface concentration of chemisorbed oxygen was found and then its interconnection with thin film conductivity for two most important grain geometry was established. It was shown that film conductivity is described by power dependence on surface concentration of oxygen in neutral form. Also we have found that the kinetic processes of gas sensing are determined by second order reactions of adsorption/desorption of oxygen. Charging and neutralization of the chemisorbed oxygen takes place in the condition of equality of their rates. Transient curves of response/recovery were calculated for various temperatures and oxygen partial pressures. The main peculiarities of experimental transient curves are coincided with results of simulation. The explanation of transient curves for Pd surface doped films is proposed. Mechanism of gas sensitivity of SnO<sub>2</sub>:Pd films assumes the indirect participation of molecular oxygen in the surface band bending due to competition with atomic oxygen on SnO<sub>2</sub> surface for adsorption centers. This mechanism also assumes the atomic oxygen spillover from catalyst to semiconductor oxide surface. © 1999 Elsevier Science S.A. All rights reserved.

*Keywords:* Thin films; Gas sensors; Oxygen sensing; Transient curves; Simulation

## 1. Introduction

In previous reports [1,2], we presented the steady-state model of thin film gas sensors (TFGS) developed based on Volkenstein's chemisorptional theory. This model has allowed to describe and calculate the main characteristics of gas sensors (GS) such as: gas sensitivity's dependencies on parameters of the films, operating temperature and concentration of detected gas (CO). In present report, we made the next step in the trend of modeling of TFGS behavior and examined the applicability of proposed chemisorptional model for the analysis of gas-sensing properties of GS in transient case, i.e., for analysis of kinetics of gas sensitivity.

Unfortunately, the present-day status in this field of study of chemical sensors remains unsatisfactory. We could refer only to a few works, devoted to only some individual aspects of this problem [3–8], but the attempts of consis-

tent approach to kinetics of sensing mechanism are still missing.

At this stage of research, we put the task to study gas sensor's behavior in oxygen atmosphere in the case of active gas absence. Without study of this process, it is difficult to interpret subsequently the kinetics of GS sensing in the presence of detected gas in the ambient atmosphere. Another substantial data for carrying out this study were the results of our experimental research [9,10]. In these experiments, we determined the both dominant role of oxygen behavior among the processes limiting the kinetics of SnO<sub>2</sub> films' gas sensitivity, and the independence of this kinetics on the nature of reducing gas (CO or H<sub>2</sub>).

## 2. Theory

### 2.1. Balance and kinetics of chemisorbed particles

The expanded equations of gas particles' balance on semiconductor surface for the neutral and charge forms of

<sup>\*</sup> Corresponding author. Fax: + 373-2-248378; e-mail: koro@ch.moldpac.md

chemisorbed oxygen [11] are the basis of our theoretical study

$$dN_O^o/dt = \alpha_o P_{O_2} (N^* - N_O)^2 - \beta_o (N_O^o)^2 - \beta_1 N_O^o + \beta_2 N_O^- \quad (1)$$

$$dN_O^-/dt = \beta_1 N_O^o - \beta_2 N_O^- \quad (2)$$

where  $N^*$  and  $N_O$  are the total number of adsorption centers and oxygen atoms on the surface, respectively;  $N_O^o$  and  $N_O^-$  are the number of oxygen atoms in neutral and charged forms;  $P_{O_2}$  is the partial pressure of oxygen in gas phase;  $\alpha_o$ ;  $\beta_o$  are the coefficients of adsorption and desorption; and  $\beta_1$ ;  $\beta_2$  are the coefficients of charging and neutralization of chemisorbed oxygen.

Due to the dissociative character of oxygen chemisorption on  $SnO_2$  surface in analyzed range of temperatures ( $> 250^\circ C$ ), we used the second-order rate equations for describing surface chemical reactions. Also we had been assumed the absence of lateral interaction between chemisorbed particles.

As in our last works [1,2], we have considered the case of quasi-continuous distribution of Gauss-type of chemisorbed states in the band gap. This significant feature has the principal importance for describing of gas sensor characteristics. This fact can be illustrated, for example, for the surface potential dependence on partial pressure in steady-state case.

### 2.1.1. Surface potential of $SnO_2$ in oxygen atmosphere

It is well known that surface potential is determined by oxygen adsorbed on the surface in charge form. Relationship between charged and neutral forms of adsorbed oxygen can be written in the form [1]

$$N_O^- = \frac{N_O}{\sqrt{2\pi}\sigma_O} \int \frac{\exp\left[-\frac{(U_O - U_O^M)^2}{2\sigma_O^2}\right] dU_O}{1 + \exp\left(\frac{U_S + E_V - U_O^M}{\varphi_T}\right)} = N_O I_o \quad (3)$$

where

$$N_O = N_O^- + N_O^o, \quad N_O^o = N_O^- (1/I_o - 1) \quad (4)$$

and  $E_V$  is the bulk Fermi level position;  $U_O^M$  = position of maximum of distribution of oxygen chemisorbed level;  $\sigma_O$  = dispersion of oxygen level distribution; and  $\varphi_T$  = temperature potential. All energetic positions are determined from the bottom of conduction band. In a wide range of surface potential values ( $U_S$ ), integral  $I_o$  is close to

$$I_o \approx 1/\left[1 + \exp(U_S + E_V - U_O^M)/E^*\right] \quad (5)$$

where

$$E^* = \varphi_T + K\sigma_O, \quad K \approx 0.3-0.5 \quad (6)$$

Numerical calculations confirm this interesting feature which, in a general case, is correct not only for chemisorbed levels. For the discrete distribution ( $E^* = \varphi_T$ ) of chemisorbed states, the relationship between total value of neutral and charged forms is described by Fermi distribution. We have to emphasize that in the case of continuous distribution of chemisorbed states, the relationship between the densities of energy states of chemisorbed forms  $N_O^o(U_O)$  and  $N_O^-(U_O)$  also remains of Fermi-type. Using Eqs. (4) and (5), one can get

$$N_O^o = N_O^- \exp(U_S + E_V - U_O^M)/E^* \quad (7)$$

Taking into account both Eqs. (1) and (7) in steady-state case (i.e.,  $dN_O^o/dt = 0$ ;  $dN_O^-/dt = 0$ ) and Schottky equation for surface potential, it is easy to make up the expression for the surface potential:

$$U_S = U_O^M + E_V + 1/2 E^* \ln \tau_d/\tau_a + C \cong \text{const} + E^* \lg P_{O_2} \quad (8)$$

where

$$\tau_a = 1/(\alpha_o P_{O_2} N^*), \text{ and } \tau_d = 1/(\beta_o N^*) \quad (9)$$

and  $C$  is some term independent on  $P_{O_2}$ .

As it will be shown further,  $\tau_a$  and  $\tau_d$  are the time constants, connected with adsorption and desorption processes. Thus, if  $P_{O_2}$  changes on the one decade ( $P_{O_2}^{(1)}/P_{O_2}^{(2)} = 10$ ) then  $\Delta U_S = E^*$ . In the case of discrete distribution of chemisorbed states, we have  $\Delta U_S = \varphi_T$ .

### 2.1.2. Kinetics of chemisorbed particles

The mathematical difficulty of the solution of Eqs. (1) and (2) is stipulated by the facts that Eqs. (1) and (2) are nonlinear, and  $\beta_1$ ,  $\beta_2$  are dependent on surface potential. Moreover, in a general case, it is necessary to introduce Fermi quasi-level for oxygen chemisorbed states, because of absence of equilibrium between charging and neutralization of surface oxygen.

Analyzing the parameters  $\beta_1$  and  $\beta_2$ , we can conclude that only  $\beta_2$  is determined by the Fermi quasi-level, because the probability of electron injection to conduction band is determined by  $N_O^-(U_O)$  distribution, which is connected with Fermi quasi-level position. If the oxygen capture cross-section is independent on energetic position of  $O^-$ ,  $\beta_1$  is determined by Fermi level position for conduction electrons. Taking into account, that written expressions for  $\beta_2$  are remained the same as in steady-state case ( $\beta_2 = \beta_1(1/I_o - 1)$ ) and changing the Fermi level position on quasi-level position, one can write

$$\beta_2 = a_1 N_C \exp\left[-\frac{(U_S + E_V + \Delta F)}{\varphi_T}\right] \left(\frac{1}{I_o^-} - 1\right) \quad (10)$$

and then

$$\begin{aligned} \beta_2 N_{O^{\circ}} &= \beta_1 \exp\left(-\frac{\Delta F}{\varphi_T}\right) N_{O^{\circ}} \left(\frac{1}{I_{O^{\circ}}} - 1\right) \\ &= \beta_1 N_{O^{\circ}} \exp\left(-\frac{\Delta F}{\varphi_T}\right) \end{aligned} \quad (11)$$

where  $\Delta F$  = the difference between Fermi level position for the electrons and Fermi quasi-level position for chemisorbed states;  $I_{O^{\circ}}$  = non-equilibrium integral in the transient case (we must introduce  $U_S + E_V + \Delta F$  instead  $U_S + E_V$  in Eq. (3) and  $\beta_1 = a_1 n_S$ , where  $a_1$  = rate constant of electron capture at oxygen level;  $n_S = N_C \exp(-(U_S + E_V)/\varphi_T)$  = electron surface concentration; and  $N_C$  = effective density of conduction band states.

If we use the Eq. (7) approximation instead of Eq. (4) on the basis of Eqs. (1) and (2), one can get such system of equations

$$\frac{dN_{O^{\circ}}}{dt} = \alpha_o P_{O_2} (N^* - N_{O^{\circ}})^2 - \beta_o (N_{O^{\circ}})^2 - \frac{dN_{O^{\circ}}}{dt} \quad (12)$$

$$\frac{dN_{O^{\circ}}}{dt} = \beta_1 N_{O^{\circ}} \left[ 1 - \exp\left(-\frac{\Delta F}{\varphi_T}\right) \right] \quad (13)$$

$$\Delta F = E^* \ln\left(\frac{N_{O^{\circ}}}{N_{O^{\circ}}}\right) + U_{O^M} - E_V - U_S \quad (14)$$

One can see from Eqs. (12)–(14) that there are two subsystems that determine the balance of particles and transient processes on SnO<sub>2</sub> surface. The first subsystem is gas phase  $\leftrightarrow$  neutral surface oxygen. The kinetics of the neutral oxygen transfer between gas phase and SnO<sub>2</sub> surface is determined by adsorption/desorption processes and its mathematical form is presented by Eq. (12). The second subsystem is conduction electron  $\leftrightarrow$  chemisorbed oxygen. The kinetics of electron transfer between conduction band and chemisorbed oxygen is determined by the physical processes of charging/neutralization of chemisorbed oxygen by electrons and described by Eq. (13).

Numerical modeling shows that essential deviation from quasi-equilibrium ( $\Delta F \neq 0$ ) is possible when

$$\tau^{\circ} \gg \tau^* \text{ and } \tau^{-} \gg \tau^*,$$

$$\text{where } \tau^{\circ} = 1/\beta_1; \tau^{-} = 1/\beta_2; \tau^* = \sqrt{\tau_a \tau_d} \quad (15)$$

In this case, the changing of oxygen neutral states number takes place ( $dN_{O^{\circ}}/dt \gg dN_{O^{\circ}}/dt$ ) at the beginning of transient, and only then, in condition  $N_{O^{\circ}} \approx \text{const}$ , the changing of oxygen states number in charge form  $dN_{O^{\circ}}/dt \ll dN_{O^{\circ}}/dt$  will be observed. Then the kinetics and total times of this transient will be determined by electron  $\leftrightarrow$  chemisorbed oxygen subsystem, i.e., by charging and neutralization of chemisorbed levels. However, numerical simulation has shown that for surface potential  $\leq 1.0$  eV, the discussed mechanism of transient can be observed if the cross-section of electron captured for chemisorbed oxygen does not exceed  $10^{-21} \text{ cm}^{-2}$ . Only in this case,  $\Delta F$  is sufficiently larger than  $\varphi_T$ . However, such cross-sections

are too small, as compared with effective and geometric sizes of atoms. Therefore, this situation is not physically real. So, apparently, we have the situation of quasi-equilibrium in given subsystem ( $\Delta F \rightarrow 0$ ), i.e., there is a quasi-equilibrium between neutral and charge oxygen forms. In other words, the processes of charging/neutralization of chemisorbed oxygen are fast; therefore, the subsystem gas  $\leftrightarrow$  surface neutral oxygen but not subsystem electron  $\leftrightarrow$  chemisorbed oxygen determines the kinetics of transient processes in oxygen atmosphere.

Experimental results discussed in Refs. [9,10] confirm this conclusion. In particular, we have observed the decrease of response/recovery times in well-characterized situations, in which some pretreatment were used to increase the surface potential. If the kinetics would be determined by electron  $\leftrightarrow$  charged oxygen subsystem, we should observe the increasing of response and recovery times, because  $\tau^{\circ}$  and  $\tau^{-}$  increase with  $U_S$  rise. However, we had been observed the opposite behavior of time constants of transient curves, which can be explain when kinetics is determined by surface adsorption/desorption processes. This fact, which we have established for chemisorbed particles, is analogous for well-known physical principle of quasi-equilibrium in the case of thermally stimulated conductivity, so called ‘‘Adirovich principle’’ [12]. It means that  $\beta_1 N_{O^{\circ}} \approx \beta_2 N_{O^{\circ}}; \Delta F = 0$ ; and  $dN_{O^{\circ}}/dt \gg dN_{O^{\circ}}/dt$  take place in the whole time interval of transient process observation. From this fact, one can see that Eqs. (1) and (2) become independent and can be solved analytically. As a result of such solution we obtained general form for  $N_{O^{\circ}}(t)$

$$N_{O^{\circ}}(t) = N_{O^{\circ}}(0) \frac{1 + \left[ \frac{N_{O^{\circ}}(\infty) + K}{N_{O^{\circ}}(0)} \right] \text{th} \frac{t}{\tau^*} + \frac{K}{N_{O^{\circ}}(\infty)} \left( \exp \frac{2t}{\tau^*} + 1 \right)^{-1}}{1 + \left[ \frac{N_{O^{\circ}}(0) + K}{N_{O^{\circ}}(\infty)} \right] \text{th} \frac{t}{\tau^*} + \frac{K}{N_{O^{\circ}}(\infty)} \left( \exp \frac{2t}{\tau^*} + 1 \right)^{-1}} \quad (16)$$

where

$$\begin{aligned} N_{O^{\circ}}(0) &= \frac{N^*}{1 + \sqrt{\tau_{an}/\tau_d}}; N_{O^{\circ}}(\infty) = \frac{N^*}{1 + \sqrt{\tau_a/\tau_d}}; \\ K &= -\frac{2N^*}{1 - \tau_a/\tau_d}, \end{aligned} \quad (17)$$

$N_{O^{\circ}}(0) = N_{O^{\circ}}(t)$  at  $t = 0$ ;  $N_{O^{\circ}}(\infty) = N_{O^{\circ}}(t)$  at  $t = \alpha$ , and  $\tau_{an}, \tau_a$  correspond the time constants of adsorption before and after changing of oxygen partial pressure.

Concentration of oxygen in charged form is determined by

$$N_{O^{\circ}}(t) = \beta_1/\beta_2 N_{O^{\circ}}(t) \quad (18)$$

From this expression, it is easy to get relationship for  $\beta_1/\beta_2$  if we use Eqs. (5) and (6)

$$\frac{\beta_1}{\beta_2} = \exp\left(-\frac{U_s + E_v - U_o^M}{E^*}\right) \quad (19)$$

In [1] we used another expression for  $N_o^o(t)$ , which was obtained for  $N^* \ll N_o^o$  case. General expression (16) includes this situation as a special case. Our recent numerical simulation of steady-state model showed that situation when  $N^* \sim N_o^o$ , i.e., the surface coverage is considerable, is more real. Only in this case, we were able to explain some principal moments of surface phenomena, such as:

–details of transition between molecular and atomic forms of oxygen on  $\text{SnO}_2$  surface;

–surface potential's independence on temperature in the range of low temperatures;

–the slopes of Arrhenius dependencies of conductivity; TPD experiments; and

–kinetic characteristics of surface doped  $\text{SnO}_2$ :Pd films.

One can see from Eq. (17) that for the temperature range  $T > 200^\circ\text{C}$ , where molecular form is negligible, the value of  $N_o^o$  is determined by  $\tau_a/\tau_d$  ratio (or  $\beta_o/\alpha_o P_{O_2}$ ).

## 2.2. Relationship between surface oxygen concentration and film conductivity

The next step in our modeling is finding the relationship between surface oxygen concentration and sheet film conductivity. We consider two most important cases, which describe the possible mechanism of current transport in the polycrystalline films. They are: the so-called surface trap limited conductivity mode (case I), and mode when conductivity is limited by Schottky's barrier of intergrain contacts (case II) (Fig. 1).

It is assumed that in first case film conductivity is determined by bulk part of crystallite conductivity, i.e., the resistance of intergrain contacts ( $R_C$ ) is negligible in comparison with bulk resistance ( $R_B$ ). The second case is opposite situation, when  $R_C \gg R_B$ . The first case takes place in the thin films (especially in nanocrystalline films) with the almost total depletion of conduction electrons. The second case appertains to ceramic or thick films. These cases can be compared by relationship between the crystallite size ( $D$ ) and Debye length ( $L_D$ ) of material ( $D \sim L_D$  – I case;  $D \gg L_D$  – II case). As a rule, first case takes place when  $D \leq 3L_D$ .

It is clear that in real situation, more complicated cases are observed. However, only the abovementioned cases are applied for describing the conductivity of most gas-sensitive structures used for GS design.

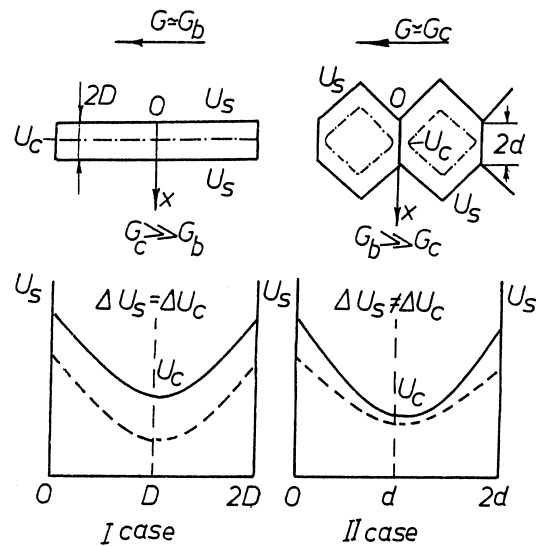


Fig. 1. Schematic illustrations for two different grain geometry corresponding to two mechanisms of electron transfer in the film, and potential distributions across the direction of current transport. ( $G_c$  and  $G_b$  correspond to parts of conductivity connected with contact and bulk). Two potential distributions under variations of ambient conditions for every case are shown.

### 2.2.1. Surface trap limited conductivity mode (case I)

This case is characterized by the following condition

$$N_s \cong 2N_d D \quad (20)$$

where  $N_s \cong N_o^-$  = surface negative charge at the top side (or one side) of crystallite (see Fig. 1),  $N_d$  = concentration of shallow donors, and  $D$  = half thickness of crystallite.

During modeling, we took into account the presence of two shallow levels (0.03 and 0.15 eV) for oxygen vacancies. More exact interval of  $N_s$  for realization of this mode is  $N_s > 2N_d(D - L_D)$  (of course  $N_s < 2N_d D$ ).

The results of our analysis are following. When shallow donors are totally ionized, the surface potential is determined as

$$U_s \cong \frac{qN_d D^2}{\epsilon \epsilon_0} + U_c = U_{sd} + U_c \quad (21)$$

where  $U_c$  = potential at the centre of crystallite;  $U_{sd}$  = the part of surface potential, which is determined by Schottky formula with  $N_s$  by Eq. (20). At that, expression for  $U_c$  is

$$U_c = -\varphi_T \ln \left[ \frac{1}{bL_D} \left( 2D - \frac{N_s}{N_d} \right) \right] \quad (22)$$

where  $b$  = some coefficient, connected with the degree of donor ionization.

It can be shown that in the conditions of total depletion of conduction electrons the surface integral of sheet conductivity has the form

$$G = 2\sqrt{\pi} q \mu N_C L_D \exp\left[-(U_c + E_v)/\varphi_T\right], \quad (23)$$

where  $\mu$  = electron mobility. One can see that Eq. (23) can be transformed to

$$G = G_0 \exp(-U_S/\varphi_T), \quad (24)$$

where

$$G_0 = 2\sqrt{\pi} q \mu N_C L_D \exp[(U_{sd} - E_V)/\varphi_T] \quad (25)$$

$U_{sd}$  is independent on gas pressure and temperature in some region where the first case is kept. Therefore, under variation of ambient conditions ( $P_{O_2}$ ,  $T$ ) we have  $\Delta U_S = \Delta U_C = \Delta U(x)$  (see Eq. (21) and Fig. 1). In other words, when ambient conditions change, the conduction band shifts equidistantly with regard to Fermi level over the grain thickness. It is the so-called ‘‘Fermi level shift’’ [3]. Typical calculated values for  $U_C$  is approximately 0.1–0.3 V for  $D \approx 10$  nm,  $N_d \sim 5 \cdot 10^{18}$  cm $^{-3}$ ,  $T = 300^\circ\text{C}$ ,  $P_{O_2} = 20\%$ . We have to emphasize that this form Eq. (24) is being correct for  $U_S > U_{sd}$ .

Of course, the full film conductivity is determined as space network of grains, and the grain surfaces can be open, close and partial open for ambient gas. We consider first case without random distribution of grain sizes. The abovementioned cases can be taken into account, if the additional multiplier, connected with geometric factor, put into the Eq. (24). From our estimations, this multiplier can be equal to 1–10. For monocrystalline films, instead of grain size, we have to use the film thickness.

### 2.2.2. Conductivity limited by intergrain Schottky contacts (case II)

The second case is well known in literature [13]. However, we would like to make its form of representation more precise.

Traditionally, the written expression for inter-grain conductivity coincides with (24). As one can see from Fig. 1, in general case, when the effective size of inter-grain contacts is comparable with  $L_D$ , some distribution of barriers potential along the contact section must be observed. This distribution is determined by the  $L_D/d_o$  ratio, where  $d_o$  is the typical size of contact. At that, the difference between  $U_S$  and  $U_C$  may be significant. Therefore, we cannot suppose the constancy of potential barriers heights on the area on inter-grain contacts. Thus, we must take into account this peculiarity in conductivity analysis.

The exact calculation of barrier potential distribution has sufficient difficulties, connected with need of decision of two-dimensional Poisson equation. At this stage of TFGS modeling, the detailed form and distribution of potential is not important to us. We can introduce some parameters, which characterize the average intercrystallite barrier height

$$U_{\text{eff}} = U_S/n, \text{ where } n \geq 1 \quad (26)$$

Then

$$G = G_0 \exp(-U_S/n\varphi_T) \quad (27)$$

One can see that expression for sheet conductivity (Eq. (27)) has the same form as in the first case. Taking into account the expression for  $U_S$  (see Eq. (14)) in condition  $\Delta F = 0$  we have

$$U_S = E^* \ln N_O^o/N_O^- + U_O^M - E_V \quad (28)$$

and substituting Eq. (28) in Eqs. (26) and (27), we can write the general expression for film conductivity

$$G = G^o [N_O^-/N_O^o]^m \quad (29)$$

In Eq. (29),  $m = E^*/\varphi_T \geq 1$  for the first case; and  $m = E^*/n\varphi_T$  for the second case. In the second case,  $m$  can be both  $< 1$  and  $> 1$ .  $G^o$ , of course, is different in these two cases.

### 2.3. Transient curves of conductivity

Proceeding from Eq. (29) we can write

$$\begin{aligned} \frac{\Delta G(t)}{\Delta G} &= \frac{G(t) - G(\infty)}{G(0) - G(\infty)} \\ &= \frac{[N_O^-(t)/N_O^o(t)]^m - [N_O^-(\infty)/N_O^o(\infty)]^m}{[N_O^-(0)/N_O^o(0)]^m - [N_O^-(\infty)/N_O^o(\infty)]^m} \end{aligned} \quad (30)$$

The good approximation for analytical decision of Eq. (30) is  $N_O^o \approx \text{const}$ . This situation is real, especially for conductivity limited by surface trap (case I). In this mode  $\Delta G(t)/\Delta G$  is completely determined by concentration of neutral oxygen form  $N_O^o(t)$ . However, during numerical calculations we used Eq. (18) for describing  $N_O^-(t)$ , taking into account the ordinary Schottky formula for  $U_S$ .

On the basis of the proposed model and the results of modeling, we can note some significant features of transient curves of gas sensors.

(1) Gas sensitivity kinetics in oxygen atmosphere is determined by kinetics of adsorption/desorption processes of chemisorbed oxygen in neutral form.

(2) The transient curves for both cases of film conductivity have the same form. Difference consists in parameter  $m$  only.

(3) The time constants for  $\Delta G(t)$  and  $N_O^o(t)$  curves  $\sim \tau^* = \sqrt{\tau_a \tau_d}$ . However, the time constants of kinetics of adsorption/desorption for neutral form of oxygen and for film conductivity transient do not coincide, because there is the nonlinear connection between  $N_O^o$  and  $G$  (see Eq. (29)). Dispersion of oxygen level, and distribution of potential barrier heights along inter-grain interface determine the amount of this nonlinearity.

(4)  $\tau_a \propto 1/P_{O_2}$ , whereas  $\tau^* \propto 1/\sqrt{P_{O_2}}$ . We have to note that  $P_{O_2}$  is the pressure at  $t > 0$ . At  $t = 0$  the changing of oxygen partial pressure takes place. Therefore, we sign  $P_{O_2}(O^-)$  for  $t < 0$ , and  $P_{O_2}(O^+)$  for  $t > 0$ .

(5) The ratio  $\tau^*(\text{res})/\tau^*(\text{recov}) \sim \sqrt{P_{\text{O}_2}^{\text{atm}}/P_{\text{O}_2}}$ , where  $P_{\text{O}_2}^{\text{atm}}$  is the partial oxygen pressure in ambient atmosphere, and  $P_{\text{O}_2}$  is the lower level of partial pressure in response/recovery cycle, so  $\tau_{\text{res}}^* > \tau_{\text{recov}}^*$ .

(6) The Activation energy of temperature dependence of time constants  $\tau^*$  is equal  $1/2(E_a + q_{\text{O}_2})$ , because  $\tau^* \sim 1/\sqrt{\alpha_0 \beta_0}$ , where  $\alpha_0 = \alpha/N^* \exp(E_a/kT)$ ;  $\beta_0 = \beta/N^* \exp(q_{\text{O}_2}/kT)$ , and  $E_a$ ,  $q_{\text{O}_2}$  are activation energies of adsorption and desorption, respectively.

(7) Steady-state values of  $N_{\text{O}}^0$  are determined by expression (17) and dependent on the ratio  $\tau_a/\tau_d$ .

(8) It can be shown from general expression for  $N_{\text{O}}^0(t)$  (Eq. (16)) that there are regions of small times ( $t < 0.1-0.3\tau^*$ ), where for sufficiently large changing of oxygen partial pressure,  $N_{\text{O}}^0(t)$  has forms

$$N_{\text{O}}^0(t)(\text{recovery}) = N_{\text{O}}^0(0) \left[ 1 + (N^*/N_{\text{O}}^0(0))(t/\tau_a) \right] \quad (31)$$

$$N_{\text{O}}^0(t)(\text{response}) = \frac{N_{\text{O}}^0(0)}{\left[ 1 + (N_{\text{O}}^0(0)/N^*)(t/\tau_d) \right]} \quad (32)$$

For these conditions, the kinetics is determined by only adsorption or only desorption processes with time constants  $\tau_a$  and  $\tau_d$ , respectively. In the region of large times of transient, the combined mechanism of interaction of both processes of adsorption and desorption takes place, and the time constant is  $\tau^*$ .

These expressions can be obtained also by solving the kinetic equations only for adsorption or desorption.

### 3. Results of simulation and comparison with experiment

#### 3.1. Parameters for modeling and samples for experiment

For metal oxide systems and in particular for  $\text{SnO}_2$ , the present knowledge about numerical values of adsorption/desorption parameters is sufficiently poor. We were forced to use any information concerning to this question. Some estimations were made by direct cheating of thermodesorption spectra (TDS) and conductivity kinetics measurements given in various works [14–17]. We chose the more probable ranges of values of  $E_a$  and  $q_{\text{O}_2}$  as  $E_a \sim 0.5-0.6$  eV; and  $q_{\text{O}_2} \sim 2.0-2.5$  eV. The  $\alpha$  and  $\beta$  pre-exponent multipliers were estimated according to Ref. [18] in assumption of immobile adsorption layer. Their values were chosen from the range  $\alpha \sim 0.01-0.1$  m<sup>2</sup>/Vs; and  $\beta \sim 10^{14}-10^{15}$  s<sup>-1</sup>.

Other parameters used in the model were:  $N_c = 1.8 \times 10^{20}$  cm<sup>-3</sup>;  $N_d = 5 \times 10^{18}$  cm<sup>-3</sup>;  $D = 10$  nm;  $\mu = 10$  cm<sup>2</sup>/Vs;  $\varepsilon = 12$ ;  $N^* = 10^{14}$  cm<sup>-2</sup>;  $\sigma_0 = 0-0.3$  eV;  $U_{\text{O}}^M = 0.9$  V;  $a_1 = 10^{-9}$  cm<sup>-3</sup>/s.

For experimental measurement of kinetic characteristics of gas sensors, we used undoped and Pd-doped  $\text{SnO}_2$  films. These films were deposited on alumina substrates by

spray pyrolysis method. The technology of  $\text{SnO}_2$  deposition is described in Refs. [19–21]. Films had the thickness equal to 40–120 nm and concentration of electrons equaled  $(5-10) \times 10^{18}$  cm<sup>-3</sup>.

The transient curves of  $\text{SnO}_2$  conductivity were measured using the measurement cycles air  $\Rightarrow$  0.5%O<sub>2</sub> + N<sub>2</sub>  $\Rightarrow$  air and air  $\Rightarrow$  0.5%CO + air  $\Rightarrow$  air.

#### 3.2. Peculiarities of experimental transient curves

One can note some significant features of  $\sigma(t)$  experimental dependencies (see Figs. 2 and 3).

(1) The response transient curves are close to exponential form, whereas for the recovery ones are characterized by the deviation from this form of dependence.

(2)  $\tau(\text{response}) \gg \tau(\text{recovery})$ . Their ratio ( $\tau_{\text{res}}/\tau_{\text{recov}}$ ) is approximately equal to  $(P_{\text{O}_2}(+)/P_{\text{O}_2}(-))^{1/2} = (21\%/0.5\%)^{1/2}$  (these pressures were used in experiment).  $P_{\text{O}_2}(-)$  is the initial oxygen partial pressure, and  $P_{\text{O}_2}(+)$  is the final oxygen partial pressure at the step changing of surrounding gas atmosphere.

(3) Activation energies of Arrhenius curves for response time constants (see Fig. 7) is  $\sim 1.27$  eV. For recovery characteristics,  $E_{\text{act}}$  is dependent on time interval of transient observation.  $E_{\text{act}}$  equals  $\sim 1.02$  eV at middle and long times of transient, and activation energy equals 0.7 eV at short times of transient.

#### 3.3. Simulation of $N_{\text{O}}^0$

The transient curves of  $N_{\text{O}}^0$  at step changing of partial oxygen pressure are shown in Fig. 4 (lower values of pressure are given in Fig. 4). One can see that the maximum changing of  $N_{\text{O}}^0$  is observed in conditions when the lower pressure level is vacuum. At these conditions (measurement cycle air  $\Rightarrow$  vacuum  $\Rightarrow$  air) there is the minimum

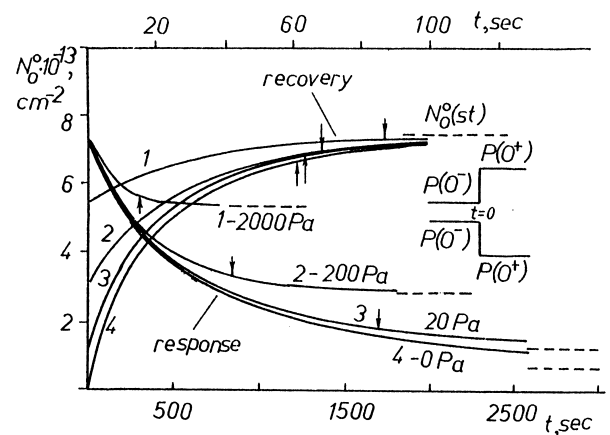


Fig. 2. Experimental (a) and theoretical (b) kinetic characteristics of film's conductivity in measurement cycle air  $\Rightarrow$  0.5%O<sub>2</sub> + N<sub>2</sub>  $\Rightarrow$  air for various temperatures: (1) 300°C; (2) 318°C; (3) 350°C; (4) 376°C ( $\alpha_0 = 0.05/N^* \exp(-0.5/\varphi_T)$ ;  $\beta_0 = 7 \times 10^{14}/N^* \exp(-2.1/\varphi_T)$ ;  $m = 1$ ).

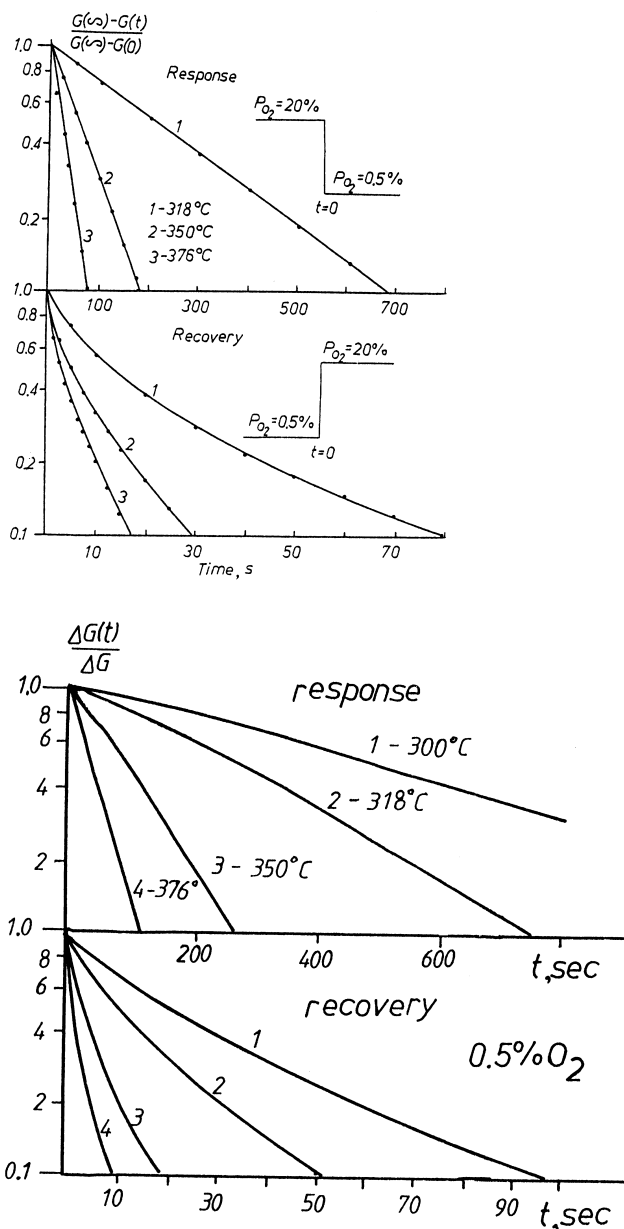


Fig. 3. Experimental and theoretical transient curves of film conductivity in measurement cycle air  $\Rightarrow$  2.5%O<sub>2</sub> + N<sub>2</sub>  $\Rightarrow$  air for various temperatures: (1) 318°C; (2) 350°C; (3) 376°C. Calculation parameters  $\alpha_{O_2}$ ,  $\beta_{O_2}$  and  $m$  are as on Fig. 2.

for recovery transient times ( $P_{O_2}(-) = 0$ ;  $P_{O_2}(+) = P_{O_2}^{atm}$ ) and there is the maximum for response transient times ( $P_{O_2}(-) = P_{O_2}^{atm}$ ;  $P_{O_2}(+) = 0$ ).

### 3.4. Simulation of $\Delta G(t)$

We made numerical simulation of transient curves with variation of parameter  $m$  (see Fig. 5 and Fig. 6), and compared obtained results with experiment. We found that good agreement with experimental dependencies was observed when  $m \leq 1$ . At  $m > 1$ , the theoretical dependencies become sufficiently nonlinear, and the  $\tau(\text{res})/\tau(\text{re-}$

cov) ratio also exceeds  $(P_{O_2}(\text{recov})/P_{O_2}(\text{res}))^{1/2}$ . Apparently, we have combined mechanism of films conductivity with the participation of two above mentioned types of conductivity limitation. It is not realistic to suppose for such films the existence of only second case of conductivity.

It was brought out also that in the frame of designed model, it is possible to estimate the parameter  $m$ , using the results of film conductivity measurement at various oxygen partial pressures. On the basis of these estimations, we got the value  $m \sim 0.7-0.8$ . At this stage of modeling, it is difficult to make any conclusions about the nature of  $m$ , i.e., what does determine its value: dispersion of oxygen level ( $E^*$ ) or parameter ( $n$ ), connected with space distribu-

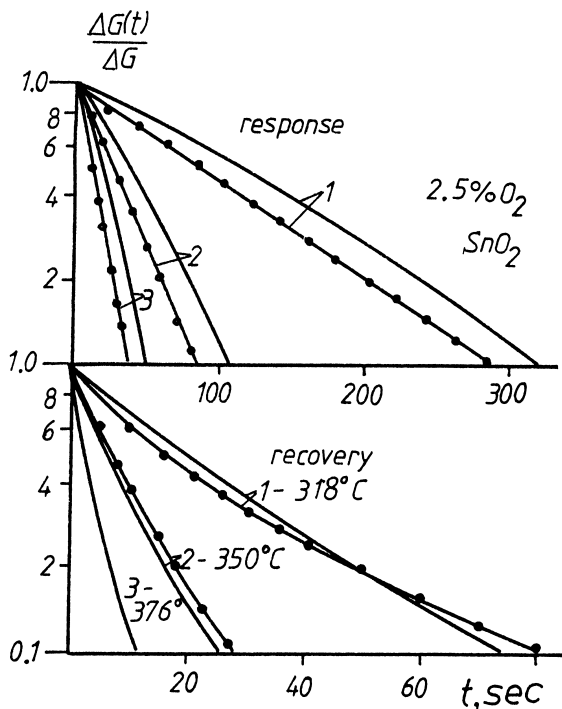


Fig. 4. Calculated transient response and recovery curves for surface oxygen concentration in neutral form for various partial pressures of oxygen in the measurement cycles air ⇒ O<sub>2</sub> + N<sub>2</sub> ⇒ air. (T = 318°C; α<sub>O</sub> = 0.05/N\* exp(-0.5/φ<sub>T</sub>); β<sub>O</sub> = 7 × 10<sup>14</sup>/N\* exp(-2.1/φ<sub>T</sub>); (1) P<sub>O<sub>2</sub></sub> = 2000 Pa; (2) 200 Pa; (3) 20 Pa; (4) vacuum. Pointers indicate the time constants of processes by the level 0.1 on total ΔN<sup>o</sup>(t) changing.

tion of potential barriers heights in the area of intercrystallite contact.

We compared also the experimental and theoretical Arrhenius dependencies of response/recovery time constants (Fig. 7). This comparison demonstrates a quite well agreement between experimental and theoretical values of both activation energies and absolute values of time constants.

### 3.5. Simulation of TDS

For verification of our model we carried out numerical simulation of TDS for the desorption parameters used in kinetics' calculations. Results of such simulation are given in Fig. 8. Desorption energy was varied in the 2.0–2.5 eV range.

One can see that maximum of theoretical thermodesorption peaks lies in the range of temperatures 430–510°C. As a rule, the temperature peaks of experimental thermodesorption spectra lie in the range 520–570°C [16]. These temperatures are somewhat higher than similar temperatures received as a result of simulation. However, indicated experimental information concerns powder specimens. For thin films, the situation may be different to some extent. For example, we have observed, in the experiment, the increase of the slope of Arrhenius dependencies of response time (E<sub>act</sub> ~ 1.6 eV) with the film thickness rise (at

the value of d > 120 nm). The nature, behavior and transformation of chemisorbed oxygen at elevated temperatures until now is not well understood and require further study.

### 3.6. Simulation of Pd doping influence

In this section, we present the preliminary theoretical results for kinetics' analysis of Pd doped SnO<sub>2</sub> thin films. Experiments on such films have showed that a high sensitivity is observed in the range of operating temperatures 100–200°C. At that, the kinetics is characterized more fast response than in case of undoped films [10]. The activation energies of Arrhenius dependencies of response/recovery times for transient curves of SnO<sub>2</sub>:Pd films are sufficiently small in comparison with analogous dependencies for undoped films [10]. For SnO<sub>2</sub>:Pd films, E<sub>act</sub> ~ 0.6–0.7 eV and 0.3 eV for response and recovery times, respectively (see Fig. 9).

One should be note that if we use the kinetic mechanism (which we used for undoped films) for describing of the process oxygen sensing by doped SnO<sub>2</sub>:Pd films, the theoretical estimations of E<sub>act</sub> and τ\* within our model will not coincide with experimental results.

It is known, that on the surface of noble metal the oxygen is in atomic form. As a rule, the dissociative chemisorption of oxygen on the Pd surface is observed already at temperatures ~ 200 K. It means that activation energy of adsorption (E<sub>a</sub>) is about to zero. At that, the activation energy of oxygen desorption from Pd surface

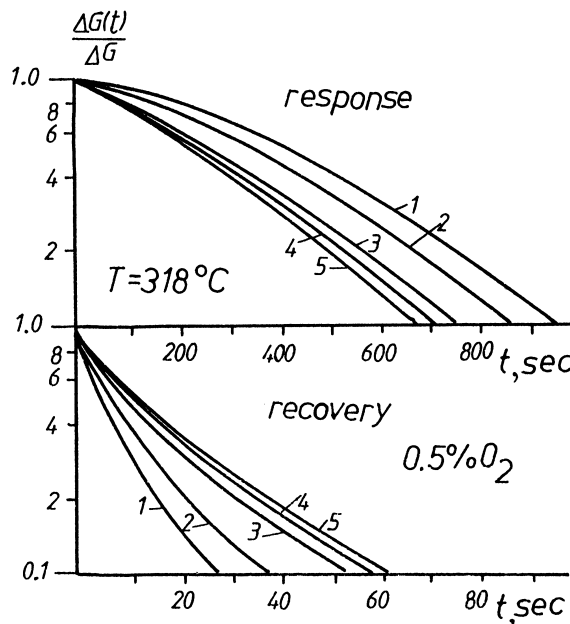


Fig. 5. Simulation of response and recovery transient curves of G(t) for different values of coefficient m. (T = 318°C; P<sub>O<sub>2</sub></sub>(res) = 0.5%). Calculation parameters α<sub>O</sub> and β<sub>O</sub> are as on Fig. 3. (1) m = 4 (σ<sub>O</sub> = 0, n = 0); (2) m = 2.5 (σ<sub>O</sub> = 0.15; n = 0); (3) m = 1 (σ<sub>O</sub> = 0; n = 0); (4) m = 0.5 (σ<sub>O</sub> = 0; n = 2); (5) m = 0.125 (σ<sub>O</sub> = 0; n = 8).

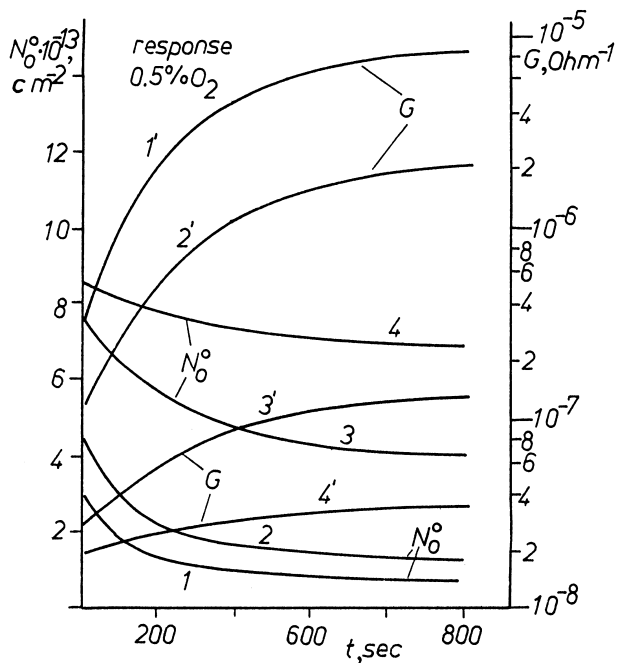


Fig. 6. Simulation of response transient characteristics for oxygen concentration  $N_0^o(t)$  and film  $G(t)$  conductivity for various values of  $\tau_a/\tau_d$  ratio ( $\tau^* = \text{constant}$ ).  $T = 318^\circ\text{C}$ ;  $P_{\text{O}_2}(\text{res}) = 0.5\%$ .

( $q_{\text{O}_2}$ ) must be not smaller than  $\sim 2.0$  eV [22]. From these facts, we can estimate the lower limit for the slope of Arrhenius dependence. In this case,  $E_{\text{act}}$  should be more than 1.0 eV. However, this is considerably larger than values of  $E_{\text{act}}$  observed in experiment.

We also observed that experimental results are very close to response/recovery times for the first order adsorption/desorption process, i.e., for molecular form of oxygen (see Fig. 9, where the results of calculations are shown). In our simulation on  $\text{SnO}_2$  surface for transfer between molecular and atomic forms near  $150^\circ\text{C}$ , we used adsorption parameters for  $\text{O}_2$  such as  $\alpha_{\text{O}_2} = 0.05 \exp(-0.3/\varphi_T)$ ;  $\beta_{\text{O}_2} = 10^{13} \exp(-1.3/\varphi_T)$ . For the first order kinetics the time constant determines as

$$\tau_1^* = \frac{\tau_{\text{al}}\tau_{\text{dl}}}{\tau_{\text{al}} + \tau_{\text{dl}}} \quad (33)$$

where

$$\tau_{\text{al}} = 1/\alpha_{\text{O}_2} P_{\text{O}_2}; \tau_{\text{dl}} = 1/\beta_{\text{O}_2} \quad (34)$$

Arrhenius dependencies of  $\tau_1^*$  for partial oxygen pressures, corresponding to response/recovery cycles are presented in Fig. 9.

Another result from our steady-state model is the essential prevailing of atomic charged oxygen form ( $\text{O}^- \gg \text{O}_2^-$ ) in this region of temperatures ( $100\text{--}200^\circ\text{C}$ ) and approximately equal amounts of neutral oxygen forms ( $\text{O}^o \approx \text{O}_2^o$ ), due to lesser depth of chemisorbed level for  $\text{O}_2^-$ . It means that film conductivity in this temperature region is determined by atomic oxygen form. However, we have to take

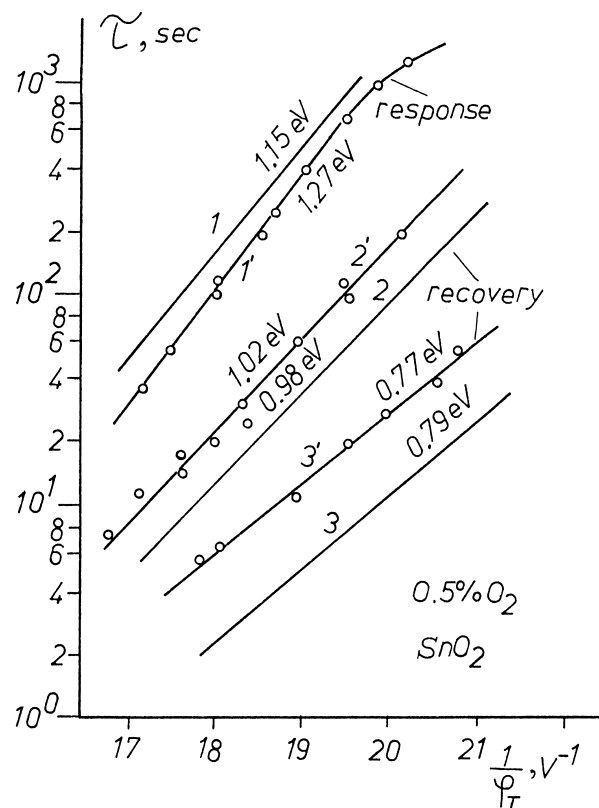


Fig. 7. Comparison of experimental and theoretical Arrhenius dependencies of response and recovery times of conductivity' transient curves.  $P_{\text{O}_2}(\text{res}) = 0.5\%$ .

into account the competition  $\text{O}_2^o$  and  $\text{O}^o$  particles at surface filling in. From this point of view, the considerable values of transient times in this temperature region for undoped samples (on order of  $\tau^* > 10^3$  s) become more understandable. This time was verified by experiment and

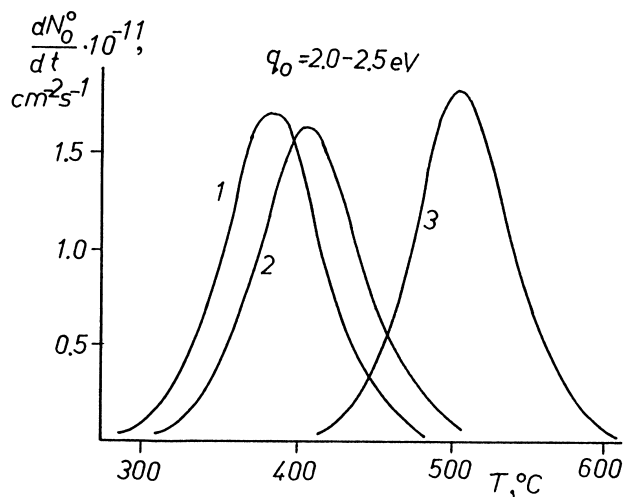


Fig. 8. Simulations of  $\text{SnO}_2$  thermodesorption spectra for various values of desorption parameter  $\beta_{\text{O}}$ : (1)  $\beta_{\text{O}} = 10^{14}/N^* \exp(-2.1/\varphi_T)$ ; (2)  $\beta_{\text{O}} = 3 \times 10^{13}/N^* \exp(-2.1/\varphi_T)$ ; (3)  $\beta_{\text{O}} = 10^{14}/N^* \exp(-2.5/\varphi_T)$ .

simulation. For undoped films, second-order adsorption/desorption rates are the slowest.

In the presence on SnO<sub>2</sub> surface of such catalyst as Pd, we have opposite situation, and the rates first-order adsorption/desorption processes are the most slowly ( $\tau_1^* \gg \tau_{II}^*$ ).

We can propose the next mechanism of kinetics for doped films in the oxygen atmosphere.

(1) Dissociative adsorption occurs practically only on catalyst surface.

(2) We suppose the spillover effect of oxygen on SnO<sub>2</sub> surface with Pd catalyst.

(3)  $V_{II}; V_{sp} > V_I$ . It means that rates of second-order adsorption/desorption processes on metal surface and diffusion of atomic oxygen from catalyst to oxide surface exceed the rate of first-order adsorption/desorption processes. Therefore, in transient process  $V_I$  determines the total rate of process.

(4) The surface coverage of SnO<sub>2</sub> by oxygen is determined by competition of its two neutral forms — molecular and atomic. We assume that

$$N_{O_2}^o(t) \sim N^* - N_{O_2}^o(t). \Rightarrow \frac{dN_{O_2}^o}{dt} \cong - \frac{dN_{O_2}^o}{dt} \quad (35)$$

(5) Sheet film's conductivity is determined by atomic oxygen charged form on SnO<sub>2</sub> surface. Taking into ac-

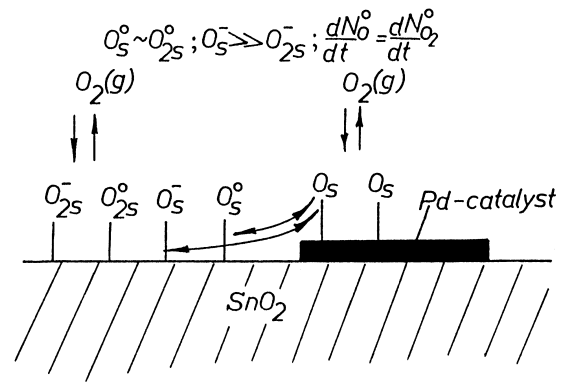


Fig. 10. Schematic illustration of surface refilling by oxygen on Pd-doped SnO<sub>2</sub> surface.

count Eqs. (29) and (35), we can suppose the first simple approximation

$$G(t) \sim [N^* - N_{O_2}(t)]^{-m} \quad (36)$$

Illustration of this mechanism is given in Fig. 10. It seems that this is the most simple explanation of observed experimental facts and do not contradict the present ideas of dominant role of surface phenomena on metal oxides in the processes of gas sensing. Of course, these results require further theoretical and experimental studying.

#### 4. Conclusions

(1) The chemisorptional model for quantitative description of the transient characteristics of metal oxide gas sensors in oxygen atmosphere without active impurities is presented.

(2) The kinetics of oxygen sensing occurs in the conditions of quasi-equilibrium between conduction electrons and chemisorbed oxygen, i.e., transient at step changing of oxygen partial pressure in ambient atmosphere takes place in conditions of almost total equality of charging and neutralization rates of chemisorbed levels. Time constants of transient curves are determined by adsorption/desorption rates of oxygen in neutral form.

(3) The film's conductivity is determined by power dependence on oxygen concentration in neutral form. Charged form of oxygen, on dependence on ambient conditions, is changed most weakly.

(4) We proposed semiquantitative explanation of experimental transient curves for Pd surface doped SnO<sub>2</sub> films. The important role of molecular chemisorbed oxygen for understanding kinetic mechanism of gas sensing is shown. Obtained results are indirect confirmation of existence of oxygen spillover on SnO<sub>2</sub> surface.

#### 5. Uncited reference

[13]

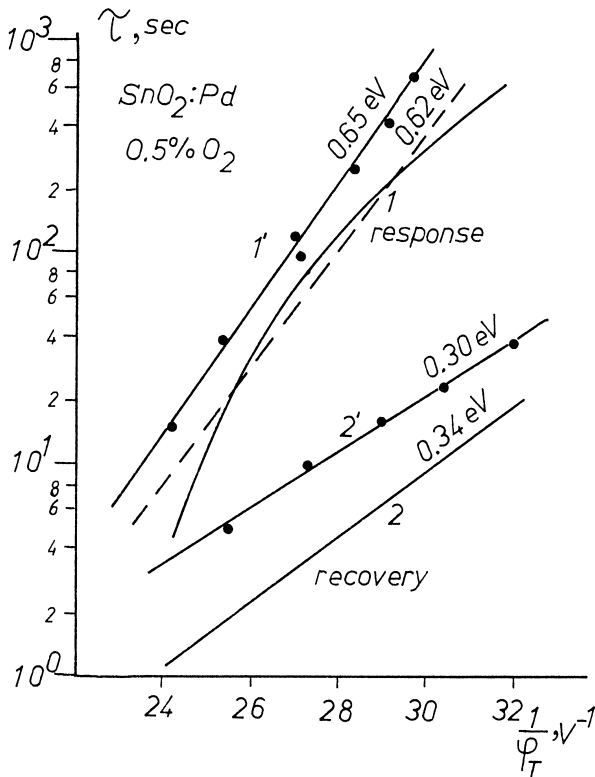


Fig. 9. Comparison of experimental and theoretical Arrhenus dependencies of response and recovery times of transient conductivity curves for surface doped SnO<sub>2</sub> films.  $P_{O_2}(\text{res}) = 0.5\%$ .

## References

- [1] V. Brynzari, S. Dmitriev, G. Korotchenkov, Chemisorptional model of thin film gas sensor, Proc. of Intern. Conf. on Solid State Transducers, EUROSENSORS XI, Vol. 1, Warsaw, Poland, 21–24 September 1997, pp. 91–94.
- [2] V. Brynzari, G. Korotchenkov, S. Dmitriev, Theoretical study of semiconductor thin film gas sensitivity: attempt to consistent approach, *J. Electron. Technol.* 32 (1999) in press.
- [3] J.W. Gardner, Electrical conduction in solid-state gas sensors, *Sens. Actuators* 18 (1989) 373–387.
- [4] N. Butta, M. Melli, S. Pizzini, Influence of surface parameters and doping on the sensitivity and on the response times of tin oxide resistive sensors, *Sens. Actuators*, B 2 (1990) 151–161.
- [5] A. Galdikas, Z. Martunas, A. Setkus, SnInO-based chlorine gas sensor, *Sens. Actuators*, B 7 (1992) 633–636.
- [6] Y.D. Varlamov, O.F. Bobrenok, M.R. Predtechensky, Study of the oxygen exchange process in La–Sr–Cu–O films at oxidation–reduction surface reactions, *Sens. Actuators*, B 31 (1996) 119–122.
- [7] I. Lundstrom, Approaches and mechanisms to solid state based sensing, *Sens. Actuators*, B 35–36 (1996) 11–19.
- [8] S.P. Golubkov, Physical principles and scheme-design peculiarities of semiconductor gas sensors, Proc. of 2nd Conf. of Soviet and Polish Young Scientist, Wroclaw, Poland, 1986, pp. 42–45.
- [9] G. Korotchenkov, V. Brynzari, S. Dmitriev, Kinetics of undoped SnO<sub>2</sub> thin film's gas sensitivity, Proc. of the 7th Intern. Meeting on Chemical Sensors, Beijing, China, July 27–30, 1998, pp. 517–519.
- [10] G. Korotchenkov, V. Brynzari, S. Dmitriev, Kinetics characteristics of SnO<sub>2</sub> thin film gas sensors for environmental monitoring, S. Buettgenbach (Ed.), SPIE, Bellingham, Proc. of SPIE. V.3539, Chemical Microsensors and Applications (1998) pp. 196–204.
- [11] F.F. Volkenstein, *The Electronic Theory of Catalysis on Semiconductors*, Pergamon, Oxford, 1963.
- [12] V.N. Vertoprahov, E.G. Salman, *Thermally Stimulated Current in Nonorganic Materials*, Science, Novosibirsk, 1979 (in Russian).
- [13] K.D. Schierbaum, U. Weimar, R. Kowalkowski, W. Gopel, Conductivity, work function and catalytic activity of SnO<sub>2</sub>-based sensors, *Sens. Actuators*, B 3 (1991) 205–214.
- [14] D. Kohl, Surface processes in the detection of reducing gases with SnO<sub>2</sub>-based devices, *Sens. Actuators* 18 (1989) 71–113.
- [15] Y. Tamaki, M. Nagaihi, Y. Teraoka, Adsorption behavior of CO and Interfering gases on SnO<sub>2</sub>, *Surf. Sci.* 221 (1989) 183–186.
- [16] M. Egashira, M. Nakashima, S. Kawasumi, Temperature programmed desorption study of water adsorbed on metal oxides: 2. Tin oxide surfaces, *J. Phys. Chem.* 85 (1987) 4125–4130.
- [17] J.F. McAleer, P.T. Mosely, J.O.W. Norris, D.E. Williams, Tin dioxide gas sensors, *J. Chem. Soc., Faraday Trans. 1* 83 (1987) 1323–1346.
- [18] Trepel, *Hemosorption*, Moscow, 1958 (in Russian).
- [19] S. Dmitriev, G. Korotchenkov, V. Brynzari, Manufacturing peculiarities of SnO<sub>2</sub> thin film gas sensors, Proc. of the 20th Intern. Conf. on Microelectronics, Vol. 2, Nis, Serbia, 12–14 September 1995, IEEE, 1995, pp. 589–592.
- [20] G. Korotchenkov, V. Brynzari, S. Dmitriev, Process development for low cost and low power consuming SnO<sub>2</sub> thin film gas sensors (TFGS), *Sens. Actuators*, B 54 (1999) 202–209.
- [21] G. Korotchenkov, V. Brynzari, S. Dmitriev, SnO<sub>2</sub> films for thin film gas sensors design, *J. Mater. Sci. Eng. B* 63 (3) (1999) 195–204.
- [22] I. Toyoshima, G.A. Somorjai, Heats of chemisorption of O<sub>2</sub>, H<sub>2</sub>, CO, CO<sub>2</sub> and N<sub>2</sub> on polycrystalline and single crystal transition metal surfaces, *Catal. Rev.* 19 (1979) 105–159.

Ghenadii Korotchenkov received his PhD in Physics and Technology of Semiconductor Materials and Devices from Technical University of Moldova in 1976 and his Habilitate Degree in Physics and Mathematics from Academy of Science of Moldova in 1990. He is a leader of scientific group and manager of various scientific and engineering projects carried out in Department of Microelectronics, Technical University of Moldova. Dr. Habilitate G. Korotchenkov is the author of four books, more than 120 articles and 14 patents. He presented more than 80 reports on the national and international conferences. His present research interests include material sciences, focusing on metal oxide film deposition; surface science; and thin film gas sensor design.

Vladimir Brynzari received his PhD in Physics and Mathematics from State University of Moldova in 1990. He has worked in the field of optoelectronics and nonlinear optics of laser diodes from 1982 to 1990. He is a principal scientific researcher in department of microelectronics of Technical University of Moldova. His current field of interests have been focused on device simulation of thin film gas sensors.

Serghei Dmitriev received Dipl. Phys. Degree from the State University of Moldova in 1981 and MSc degree in engineering from the Technical University of Moldova in 1991. He worked as researcher in Physical Department and Specialized Technological Construction Bureau of Optoelectronics of State University of Moldova from 1981 to 1985. Since 1991, he has been the senior scientific researcher of the Lab. of Microelectronics of the Technical University and his research interests include materials and technology of semiconductor metal oxide film deposition.